



Improving CO₂/N₂ and CO₂/H₂ Selectivity of Hypercrosslinked Carbazole-Based Polymeric Adsorbent for Environmental Protection

Pegah Najafi^a, Hamid Ramezanipour Penchah^b, Ahad Ghaemi^{a,*}

- a. School of Chemical, Petroleum and Gas Engineering, Iran University of Science and Technology (IUST), Tehran, Iran
b. Department of Chemical Engineering, University of Guilan, Rasht, Iran

Received: 23 May 2020 ,Revised: 09 October 2020 Accepted: 10 October 2020
© University of Tehran 2020

Abstract

In this study, carbazole-based hypercrosslinked polymer (HCP) adsorbent was synthesized using the knitting method by Friedel-Crafts reaction. The effects of crosslinker to carbazole ratio and synthesis time on the adsorbent structure were investigated to improve CO₂/N₂ and CO₂/H₂ selectivity. Crosslinker to carbazole ratio and the synthesis time was considered in the range of 1-4 (mol/mol) and 8-18 (h), respectively. HCP adsorbents were analyzed by energy-dispersive X-ray spectroscopy (EDS), Fourier-transform infrared spectroscopy (FTIR), and Brunauer-Emmett-teller analysis (BET). The adsorption capacity of CO₂, N₂, and H₂ were measured by carbazole-based HCP and it was correlated with the nonlinear form of the Langmuir isotherm model. The achieved BET surface area of adsorbent with the highest amount of synthesis parameters was 922 (m²/g). The ideal adsorbed solution theory (IAST) was utilized to anticipate CO₂/N₂ and CO₂/H₂ selectivity at 298 k and 1 bar. CO₂/N₂ and CO₂/H₂ selectivity for adsorbent with the maximum amount of synthesis parameters were 8.4 and 4.4, respectively. The high selectivity values of carbazole-based HCPs are due to the presence of nitrogen atoms in the adsorbent structure and a more robust interaction between CO₂ molecules and the adsorbent surface.

Keywords:

Adsorption,
CO₂/H₂,
CO₂/N₂,
Hypercrosslinked polymer,
Selectivity

Introduction

Over the past century, the atmospheric concentration of greenhouse gases emitted by human activities has grown significantly. This progressive growth imposes a direct effect on global warming, and CO₂ is introduced as the major contributor [1]. Hence, the extension of reasonable technologies to carbon capture and storage (CCS) is required to reduce CO₂ emissions [2-6]. The cost of capturing and separating CO₂ is about 75% of the total cost of emissions control [7,8]. Therefore, it is essential to selective adsorption of CO₂ from N₂ in the post-combustion process or from a fuel gas stream (CH₄ or H₂) in the pre-combustion process to decrease operating costs. Thus, the selectivity of CO₂ over N₂, H₂, and CH₄ is the most important parameter to choose an adsorbent. This method has been considered due to its being corrosion-free, easy to control, and environmentally friendly [9,10]. Aqueous amines recall the need for alternative technologies due to high regeneration and recovery costs and loss of effectiveness over time [5,11-13]. An inexpensive alternative technology is physical sorption with solid adsorbents such as activated carbon [14], zeolite [15], metal-organic frameworks (MOF), and microporous organic polymers (MOP) [16]. MOPs include hypercrosslinked polymers (HCPs),

* Corresponding author:
E-mail: aghaemi@iust.ac.ir (A. Ghaemi)

polymers of intrinsic microporosity (PIMs), conjugated microporous polymers (CMPs), and covalent organic frameworks (COFs). Large surface area, low density, high physical, chemical, and thermal stability, variety of synthesis methods, and cost-effectiveness are important advantages of HCP adsorbents in the CO₂ adsorption process [17,18]. There are several strategies to attain high CO₂/N₂ selectivity, such as increasing the isosteric heat of adsorption, incorporating open metal sites, post-synthetic modification [3], and incorporating CO₂-philic functional groups in the structure of polymers [19]. Incorporating heteroatoms such as oxygen, nitrogen, sulfur, and phosphorus in the structure of polymers could enhance CO₂ selectivity [20]. Based on the literature review, selectivity (CO₂/N₂) increased by including N-rich functional groups such as amine [21-23] or N-rich heterocycles with electron-rich nature in the structure such as triazine and carbazole that enhanced CO₂-philicity [24]. In 2011, Li et al. introduced the 'knitting' strategy to synthesize HCPs which formaldehyde dimethyl Acetal (FDA) reacts with various aromatic monomers as an external crosslinker [18,25]. Saleh et al. reported six heterocyclic microporous polymers with constant synthesis parameters (synthesis time and crosslinker ratio) in the presence of FeCl₃ catalyst using the Friedel-Crafts reaction [19]. In this research, the elevated CO₂/N₂ and CO₂/H₂ selectivity were obtained at 273 K and 1 bar for carbazole-based HCP in the mixture of CO₂:N₂ = 15:85 and CO₂:H₂ = 20:80, and the potential of this adsorbent was investigated for CO₂ adsorption. Besides, the effect of synthesis parameters was examined to improve CO₂/N₂ and CO₂/H₂ selectivity of carbazole-based HCP. The ideal adsorbed solution theory (IAST) in conjunction with the nonlinear form of Langmuir pure-component isotherm model was utilized to predict the adsorption of CO₂, H₂ and N₂ and selectivity of CO₂/N₂ and CO₂/H₂ at 1 bar and 298 K.

Experimental

Materials

All chemical materials were purchased from Merck Company (Germany), including Carbazole (%97.8), formaldehyde dimethyl Acetal (%98), 1, 2-dichloroethane (%99), iron (III) chloride (%98), and ethanol (%99). Gases including H₂ (%99.9), N₂ (%99.8) and CO₂ (%99) were used in the adsorption process.

Adsorbent Synthesis

In general, Adsorbents synthesis was carried out based on the method of Li et al. [26] according to Table 1. Typically, carbazole (0.01 mol) was dissolved in 25 ml dichloroethane (DCE) at room temperature for 30 min. Formaldehyde dimethyl acetal (FDA) with a specific value (Table 1) as a crosslinker and iron chloride (III) (according to crosslinker ratio) was added to this solution. The resulting mixture was stirred at 80 °C at a specific synthesis time (Table 1) on the reflux condition. Then, the sample was filtrated and washed with distilled water and ethanol several times. Soxhlet extractor was applied to purify the resulting network by ethanol. Finally, drying the adsorbent was carried out at 150 °C in the oven and vacuum oven, respectively, during the night.

Table 1. The synthesis conditions of carbazole-based HCPs

Sample	Monomer (mmol)	Crosslinker (mmol)	ratio	Synthesis time (h)
CHCP1	10	40	4	18
CHCP2	10	40	4	8
CHCP3	10	10	1	18

After cooling to room temperature, the solid product was collected by filtration. Then, it was washed with distilled water and ethanol to remove unused materials. A Soxhlet extractor was

used to purify the produced framework with ethanol over a night. Finally, the adsorbent was dried at 150 °C for 24 h to obtain the adsorbent powder (Fig. 1).

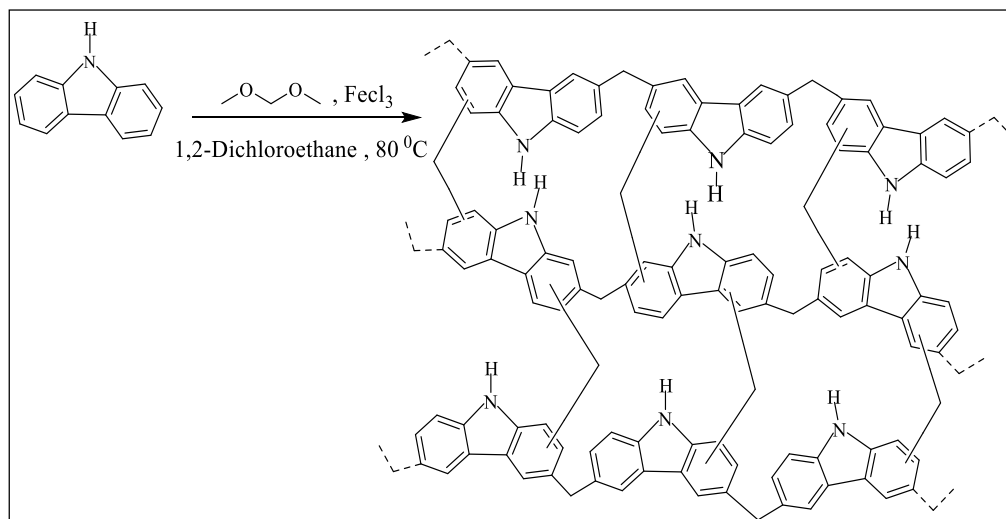


Fig. 1. final structure of carbazole-based HCP adsorbent by knitting method

Adsorption Equipment

The performance of CO₂, H₂, and N₂ adsorption was investigated in the adsorption setup (Fig. 2). The cylindrical reactor was made of stainless steel heated by a heater. The gas from the high-purity cylinder was heated after passing a heater and entered the mixing tank. The adsorbent was loaded inside the reactor to be in contact with gas and calculate the adsorption capacity. As the reactor reached the desired temperature by the heater, the gas inlet valve was opened and the gas entered the reactor from the mixing tank at the desired pressure. Also, the temperature and the pressure of the gas flowing into the reactor were measured by a thermocouple and a pressure transmitter, respectively. Mole fraction of gases in each experiment was determined by Gas chromatography. All adsorption experiments were performed with 0.5 gr adsorbent.

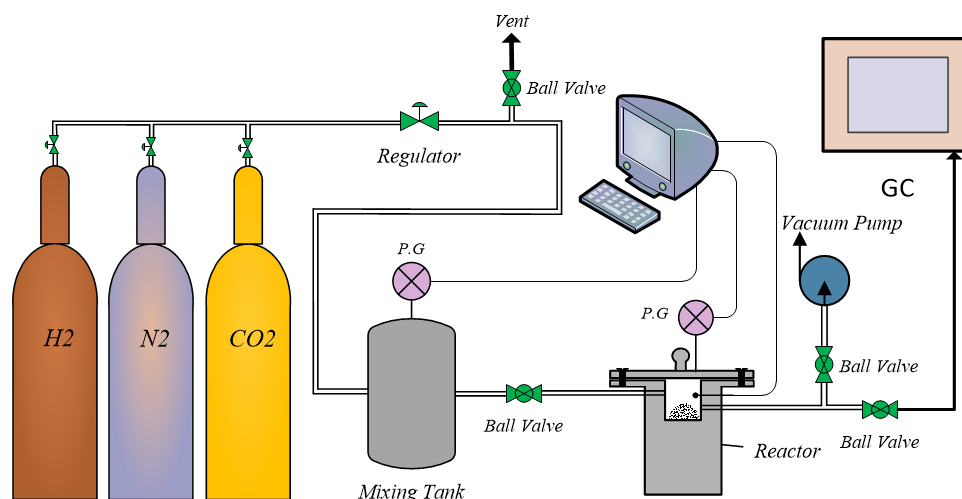


Fig. 2. Schematic of the adsorption setup

During the adsorption process, gas temperature and pressure were recorded in separate spreadsheets using the reference computer, and then, the adsorption capacity of gases was calculated by Eq. 1.

$$q = \frac{m_i - m_f}{w} = \left(\frac{VM_w}{RW} \right) \left(\frac{P_i}{Z_i T_i} - \frac{P_f}{Z_f T_f} \right) \quad (1)$$

where i and f are the initial and final conditions in the reactor, m is the mass of adsorbed gas, w is the adsorbent mass, V is the volume of the reactor, M_w is the CO₂ molecular weight, R is the universal gas constant, P is gas pressure, Z is compressibility factor, and T is gas temperature. The compressibility factor was calculated using the virial equation regardless of coefficients higher than second order. The virial coefficients were calculated by the Tsonopoulos equation.

Adsorbent Characterization Analysis

Philips-XL30 (EDS) microanalysis detector (model 6636) was used to investigate the elemental of the carbazole-based HCP. Perkin-Elmer FTIR-spectrometer was used for FTIR spectra analysis to determine the functional groups in the structure of adsorbents. Micromeritics ASAP 2020 M analyzer was used at 77.3 K for BET analysis and investigated the specific surface area of the samples.

Ideal Adsorbed Solution Theory (IAST)

The most common isotherm equation employed for modeling adsorption data is the Langmuir isotherm equation (Eq. 2), which can be used to describe the amount of material adsorbed on the adsorbent surface as a function of pressure at a constant temperature.

$$q_e = \frac{q_m b P_e}{1 + b P_e} \quad (2)$$

where q_e (mmol/g) is equilibrium adsorption capacity, q_m (mmol/g) is the maximum adsorption capacity, and b (1/bar) is the Langmuir isotherm constant [3]. In 1965, Myers and Prasnitz reported the ideal adsorbed solution theory (IAST) to anticipate mixed-gas adsorption equilibrium by pure-component adsorption isotherms. Based on their theory, there is no interaction between the molecules in the adsorbed phase, and equilibrium is achieved at a constant temperature. The Gibbs equation (Eq. 3) can be used to calculate the spreading pressure of the two-component mixed-gas [22]:

$$\int_0^{P_i^\circ} \frac{q_i}{P} dP = \frac{\pi_i A}{RT} \quad (3)$$

where A is the surface area of the adsorbent and π_i is the spreading pressure of pure-component i . Adsorbed phase is considered an ideal solution and the Raoult's law is stated as Eq. (4):

$$P y_i = P_i^\circ x_i \quad (4)$$

where x_i and y_i are the molar fraction of pure-component i in the adsorbed phase and the molar fraction of component i in the non-adsorbed mixture; P_i° is the surface pressure of pure-component i and P is the total pressure of the mixed-gas [27]. The sum of the molar fraction of component i in the adsorbed phase and molar fraction of component i in the non-adsorbed phase are given by Eqs. 5 and 6 [27]:

$$\sum_{i=1}^n x_i = 1 \quad (5)$$

$$\sum_{i=1}^n y_i = 1 \quad (6)$$

By solving these four equations, x_i and y_i were obtained simultaneously. With the values of x_i , y_i , and P_i^o determined, Eq. 7 [22] is used to calculate the adsorption capacity and Eq. 8 is used to calculate selectivity (S).

$$\frac{1}{q_t} = \sum_{i=1}^n \frac{x_i}{q_i P_i^o} \quad (7)$$

$$S = \frac{\frac{x_A}{y_A}}{\frac{x_B}{y_B}} \quad (8)$$

where q_t (mmol/g) is the amount of mixture adsorbed, q_i^o (mmol/g) is the equilibrium amount of component i adsorbed in the adsorbent, and x_A and x_B are the molar fraction of A and B gases in the adsorbed phase which are in equilibrium with the molar fraction in the gaseous phase (y_A and y_B).

Results and Discussion

Adsorbent Characterization

The result of EDS is shown in Fig. 3 and elemental analysis is shown in Table 2. Results showing the purity of the produced adsorbent indicate the performance of the Friedel-Crafts reaction.

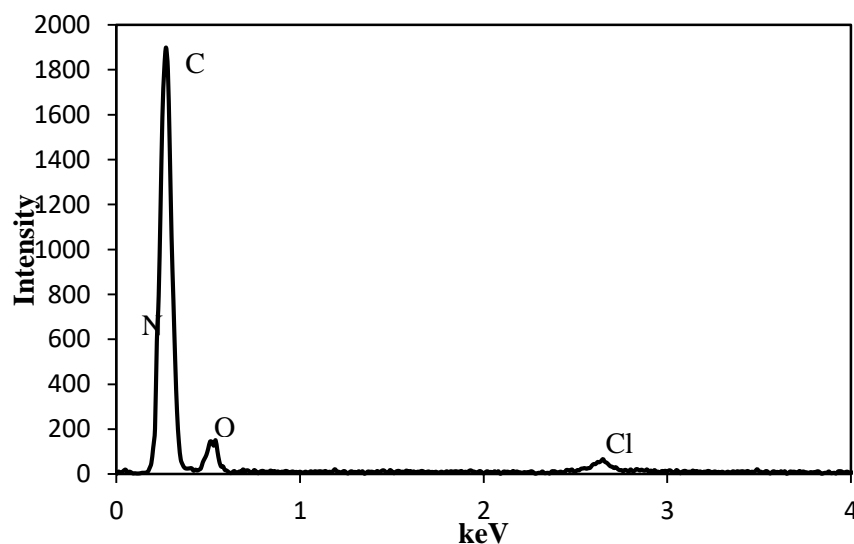


Fig. 3. EDS patterns of carbazole-based HCPs

Table 2. Elemental composition of carbazole-based HCPs

Element	Mass fraction (%)
C	69.481
N	13.822
O	16.346
Cl	0.351

Fig. 4 represents the nitrogen adsorption-desorption isotherm of carbazole-based HCP, which shows that this adsorbent has a type IV isotherm. According to IUPAC classification [23], this type of isotherm corresponds to microporous materials. Results of the BET surface area of carbazole-based HCPs with different synthesis parameters are given in Table 3.

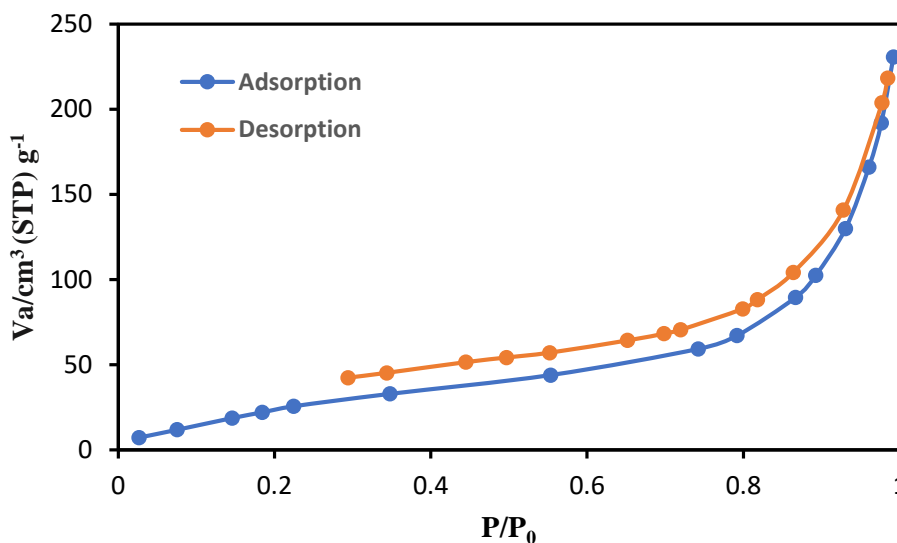


Fig. 4. BET analysis of carbazole-based HCP at 77.3 k

Table 3. BET surface area of carbazole-based HCPs

Sample	Ratio	Synthesis Time (h)	S _{BET} (m ² /g)
CHCP1	4	18	718.91
CHCP2	4	8	676.13
CHCP3	1	18	463.36

According to Table 3, the CHCP1 adsorbent with maximum values of synthesis parameters has the highest BET surface area and this value increases with increasing of crosslinker ratio at an equal synthesis time (CHCP1 and CHCP3) or with increasing of synthesis time in an equal crosslinker ratio (CHCP1 and CHCP2) which may be due to the increased Friedel-Crafts reaction between the carbazole and crosslinker in suitable synthesis time and providing more sites for the interaction between CO₂ molecules and the adsorbent. It is also clear that the crosslinker ratio is more effective than the synthesis time. Fig. 5 shows the FTIR spectra for carbazole-based HCP to investigate the functional groups of adsorbents. According to this figure, C-N, C=C, and C-Cl vibrations were shown at 1238 cm⁻¹, 1481 cm⁻¹, and 748 cm⁻¹, respectively. The peaks detected at 3420 cm⁻¹ and 1678 cm⁻¹ were due to the N-H bending and stretching vibrations, respectively. Additionally, the presence of bands at 2920 cm⁻¹ and 1323 cm⁻¹ is attributed to the C-H bending and stretching vibrations, respectively.

Adsorption Isotherm

As mentioned earlier, the ideal adsorbed solution theory (IAST) needs pure-component isotherm parameters [27]. In this study, the Langmuir model was applied to fit the pure-component isotherms. Adsorption of CO₂, N₂, and H₂ was performed at different pressures from 0.2 to 1 bar and a temperature of 298 K. The CO₂, N₂, and H₂ adsorption with carbazole-based HCPs were obtained by fitting experimental data into the nonlinear form of the Langmuir isotherm model (Figs. 6 and 7).

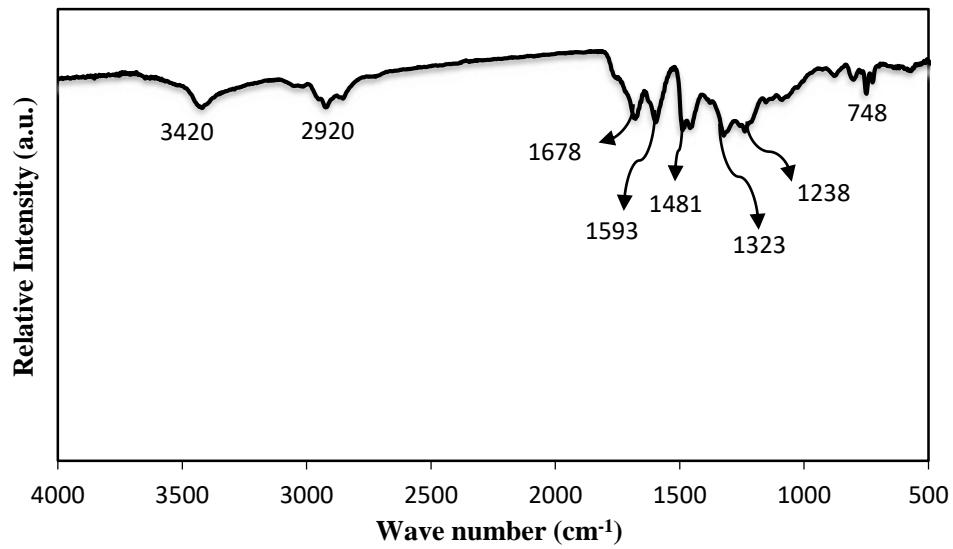


Fig. 5. FTIR spectra of carbazole-based HCP

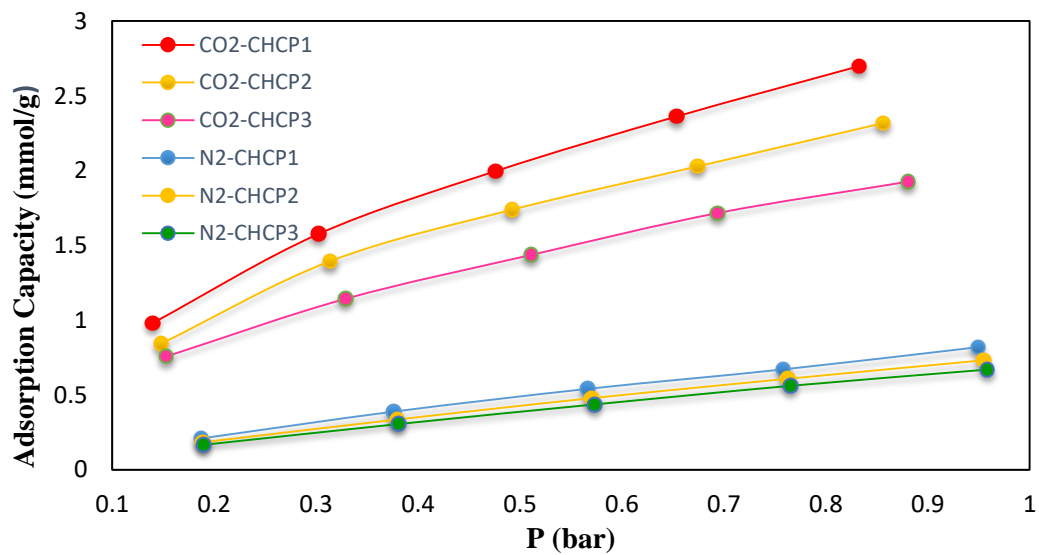


Fig. 6. CO₂ and N₂ adsorption isotherm for carbazole-based HCPs

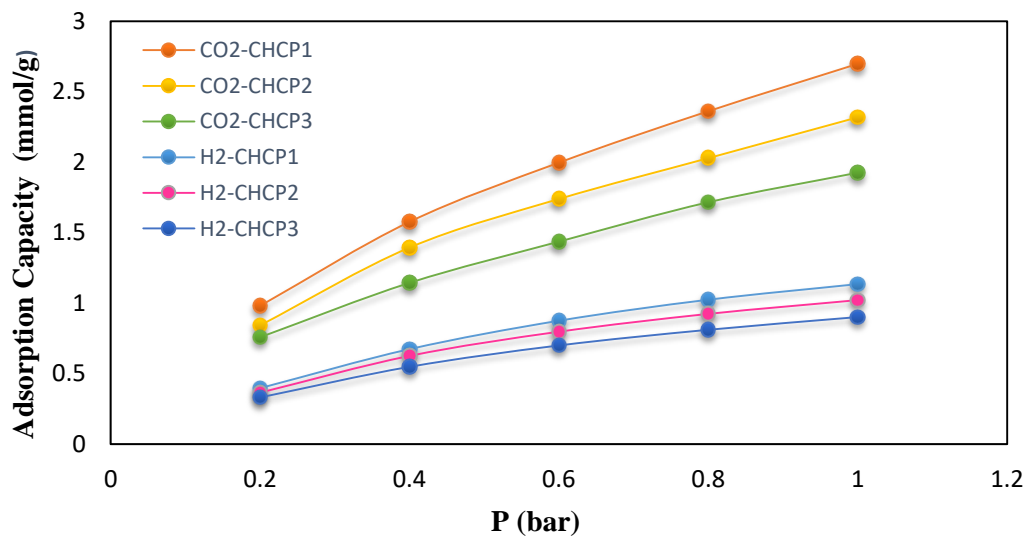


Fig. 7. CO₂ and H₂ adsorption isotherm for carbazole-based HCPs

According to the figures, CO₂ adsorption capacity on HCPs is higher than N₂ and H₂ adsorption, which can be due to the existence of nitrogen atom in the carbazole structure that creates a strong bond between CO₂ molecules and the adsorbent. Table 4 shows the values of the Langmuir isotherm parameters.

Table 4. Langmuir isotherm constants for adsorption of CO₂, H₂, and N₂ on carbazole-based HCPs

Sample	CO ₂		H ₂		N ₂	
	q _m	b	q _m	b	q _m	b
CHCP1	3.7985	2.468	2.023	1.3922	2.6706	0.4513
CHCP2	3.4243	2.1975	1.7943	1.4454	2.5224	0.4122
CHCP3	2.5729	2.6768	1.4996	1.5773	2.3776	0.3965

As shown in Table 4, with an increase in the crosslinker ratio at an equal synthesis time (CHCP1 and CHCP3) and an increase in the synthesis time at an equal crosslinker ratio (CHCP1 and CHCP2), the Langmuir parameters (q_{max} and b) increased. CHCP1, with the highest amount of synthesis parameters (ratio of 4 and synthesis time of 18 h), showed the highest values for Langmuir parameters. The b value of adsorbed CO₂ was larger than that of N₂ and H₂, which can be due to the interactive forces between adsorbent and CO₂ molecules that are bigger than the interactive forces for N₂ or H₂.

Selectivity

The selectivity of CO₂/N₂ (15:85) and CO₂/H₂ (20:80) at 298 K and 1 bar were calculated by ideal adsorbed solution theory (IAST) and the results are presented in Tables 5 and 6.

Table 5. Calculated IAST model parameters for CO₂/N₂ selectivity by carbazole-based HCPs

Sample	x _{CO2}	q _{CO2}	q _t	S
CHCP1	0.454	0.4838	1.0657	8.4073
CHCP2	0.462	0.4452	0.9637	7.7265
CHCP3	0.479	0.4321	0.9017	7.4467

Table 6. Calculated IAST model parameters for CO₂/H₂ selectivity by carbazole-based HCPs

Sample	x _{CO2}	q _{CO2}	q _t	S
CHCP1	0.456	0.6589	1.4449	4.4006
CHCP2	0.437	0.5621	1.287	3.8683
CHCP3	0.448	0.500	1.1151	3.8321

Results show that with an increase in the synthesis parameters, selectivity increases. Maximum CO₂/N₂ and CO₂/H₂ selectivity occur at maximum synthesis parameters. Because of high crosslinker ratios and synthesis time, carbazole molecules have a great opportunity to react with the crosslinker molecules and the framework is quite formed. As the results show, the effect of the crosslinker ratio on selectivity is much more than synthesis time. Selectivity is investigated by two major mechanisms, i.e. kinetic and thermodynamic of phase separation. Based on these mechanisms, the CO₂ molecule makes a stronger interaction with carbazole-based HCPs. Because CO₂ molecules with higher polarizability and quadrupole moment adsorb stronger on the surface of the adsorbent. According to the results, carbazole-based HCPs are an appropriate candidate to selectively adsorb CO₂ over N₂ or H₂. Besides, an increase in the synthesis parameters is desirable to improve CO₂/N₂ and CO₂/H₂ selectivity.

Conclusion

Three carbazole-based HCP adsorbents with different synthesis conditions (crosslinker ratio and synthesis time) were synthesized using Friedel-Crafts reaction and FDA as a crosslinker in

the presence of 1,2-dichloroethane as a solvent and FeCl_3 as a catalyst. CO_2 , N_2 , and H_2 adsorption by carbazol-based HCPs were measured at a pressure range of 0.2-1 bar and at the temperature of 298 K which fitted by the nonlinear form of Langmuir model isotherm. The selectivity of CO_2/N_2 (15:85) and CO_2/H_2 (20:80) at 1 bar and 298 K was calculated by the ideal adsorbed solution theory (IAST) model. The selectivity predicated by IAST indicated that carbazole-based HCPs were selective to CO_2 . Additionally, the effect of synthesis parameters on selectivity was studied by IAST which demonstrated that the adsorbent with the maximum amount of synthesis parameters (crosslinker ratio of 4 and synthesis time of 18 h) had maximum CO_2/N_2 and CO_2/H_2 selectivity and increasing crosslinker ratio from 1 to 4 and synthesis time from 8 to 18 h, increased adsorption capacity and selectivity of CO_2 .

Nomenclature

q	Adsorption Capacity (mmol/g)
q_e	Equilibrium adsorption capacity (mmol/g)
n	Mole of gas adsorbed
w	Mass of adsorbent (g)
R	Universal gas constant (8.314 J/mol K)
P	Pressure (bar)
P_e	Equilibrium pressure (bar)
Z	Compressibility factor
b	Constant of Langmuir isotherm
x_i	Molar fraction of the component i in the adsorbed mixture
y_i	Molar fraction of the component i in the non-adsorbed mixture
P_i°	Surface pressure of the component i (bar)
q_i°	Specific amount adsorbed of component i in the adsorbent at equilibrium (mg/g)
A	Specific surface area covered by the adsorbed mixture (m^2/g)
q_i	Specific amount adsorbed of component i in the adsorbent (mg/g)
q_t	Specific amount adsorbed of mixture (mg/g)
π_i	Spreading pressure of the component i at equilibrium

References

- [1] S. R. Reijerkerk, M. H. Knoef, K. Nijmeijer, and M. Wessling, "Poly(ethylene glycol) and poly(dimethyl siloxane): Combining their advantages into efficient CO_2 gas separation membranes," *Journal of Membrane Science*, vol. 352, no. 1, pp. 126-135, 2010/04/15/ 2010.
- [2] Y. Luo, B. Li, W. Wang, K. Wu, and B. Tan, "Hypercrosslinked Aromatic Heterocyclic Microporous Polymers: A New Class of Highly Selective CO_2 Capturing Materials," *Advanced Materials*, vol. 24, no. 42, pp. 5703-5707, 2012/11/08 2012.
- [3] H. Ramezanipour Penchah, H. Ghanadzadeh Gilani, and A. Ghaemi, " CO_2 , N_2 , and H_2 Adsorption by Hyper-Cross-Linked Polymers and Their Selectivity Evaluation by Gas-Solid Equilibrium," *Journal of Chemical & Engineering Data*, vol. 65, no. 10, pp. 4905-4913, 2020/10/08 2020.
- [4] F. Mirzaei and A. Ghaemi, "Mass Transfer Modeling of CO_2 Absorption into Blended Aqueous MDEA-PZ Solution," (in en), *Iranian Journal of Oil and Gas Science and Technology*, vol. 9, no. 3, pp. 77-101, 2020.
- [5] A. Ghaemi, "Mass Transfer Modeling of CO_2 Absorption into Blended MDEA-MEA Solution," (in en), *Journal of Chemical and Petroleum Engineering*, vol. 54, no. 1, pp. 111-128, 2020.
- [6] M. Khajeh and A. Ghaemi, "Exploiting response surface methodology for experimental modeling and optimization of CO_2 adsorption onto NaOH-modified nanoclay montmorillonite," *Journal of Environmental Chemical Engineering*, vol. 8, no. 2, p. 103663, 2020/04/01/ 2020.

- [7] C. Song, X. Xu, J. M. Andresen, B. G. Miller, and A. W. Scaroni, "Novel nanoporous" molecular basket" adsorbent for CO₂ capture," *Stud Surf Sci Catal*, vol. 153, pp. 411-416, 2004.
- [8] H. Pashaei, M. N. Zarandi, and A. Ghaemi, "Experimental study and modeling of CO₂ absorption into diethanolamine solutions using stirrer bubble column," *Chemical Engineering Research and Design*, vol. 121, pp. 32-43, 2017/05/01/ 2017.
- [9] L. Shao, S. Wang, M. Liu, J. Huang, and Y.-N. Liu, "Triazine-based hyper-cross-linked polymers derived porous carbons for CO₂ capture," *Chemical Engineering Journal*, vol. 339, pp. 509-518, 2018/05/01/ 2018.
- [10] R. Dawson, A. I. Cooper, and D. J. Adams, "Chemical functionalization strategies for carbon dioxide capture in microporous organic polymers," *Polymer International*, vol. 62, no. 3, pp. 345-352, 2013/03/01 2013.
- [11] Z. Liang, M. Marshall, and A. L. Chaffee, "CO₂ adsorption, selectivity and water tolerance of pillared-layer metal organic frameworks," *Microporous and Mesoporous Materials*, vol. 132, no. 3, pp. 305-310, 2010/08/01/ 2010.
- [12] H. Pashaei and A. Ghaemi, "CO₂ absorption into aqueous diethanolamine solution with nano heavy metal oxide particles using stirrer bubble column: Hydrodynamics and mass transfer," *Journal of Environmental Chemical Engineering*, vol. 8, no. 5, p. 104110, 2020/10/01/ 2020.
- [13] A. H. Behroozi, N. Akbarzad, and A. Ghaemi, "CO₂ Reactive Absorption into an Aqueous Blended MDEA and TMS Solution: Experimental and Modeling," *International Journal of Environmental Research*, vol. 14, no. 3, pp. 347-363, 2020/06/01 2020.
- [14] N. Karbalaee Mohammad, A. Ghaemi, K. Tahvildari, and A. A. M. Sharif, "Experimental Investigation and Modeling of CO₂ Adsorption Using Modified Activated Carbon," (in en), *Iranian Journal of Chemistry and Chemical Engineering (IJCCE)*, vol. 39, no. 1, pp. 177-192, 2020.
- [15] M. Khajeh Amiri, A. Ghaemi, and H. Arjomandi, "Experimental, Kinetics and Isotherm Modeling of Carbon Dioxide Adsorption with 13X Zeolite in a fixed bed column," (in en), *Iranian Journal of Chemical Engineering (IJChE)*, vol. 16, no. 1, pp. 54-64, 2019.
- [16] R. Dawson, T. Ratvijitvech, M. Corcoran, A. Laybourn, Y. Z. Khimiyak, A. I. Cooper, and D. J. Adams, "Microporous copolymers for increased gas selectivity," *Polymer Chemistry*, 10.1039/C2PY20136D vol. 3, no. 8, pp. 2034-2038, 2012.
- [17] C. F. Martín, E. Stöckel, R. Clowes, D. J. Adams, A. I. Cooper, J. J. Pis, F. Rubiera, and C. Pevida, "Hypercrosslinked organic polymer networks as potential adsorbents for pre-combustion CO₂ capture," *Journal of Materials Chemistry*, 10.1039/C0JM03534C vol. 21, no. 14, pp. 5475-5483, 2011.
- [18] H. Ramezanipour Penchah, A. Ghaemi, and H. Ganadzadeh Gilani, "Benzene-Based Hyper-Cross-Linked Polymer with Enhanced Adsorption Capacity for CO₂ Capture," *Energy & Fuels*, vol. 33, no. 12, pp. 12578-12586, 2019/12/19 2019.
- [19] M. Saleh, H. M. Lee, K. C. Kemp, and K. S. Kim, "Highly Stable CO₂/N₂ and CO₂/CH₄ Selectivity in Hyper-Cross-Linked Heterocyclic Porous Polymers," *ACS Applied Materials & Interfaces*, vol. 6, no. 10, pp. 7325-7333, 2014/05/28 2014.
- [20] R. Babarao, S. Dai, and D.-e. Jiang, "Functionalizing Porous Aromatic Frameworks with Polar Organic Groups for High-Capacity and Selective CO₂ Separation: A Molecular Simulation Study," *Langmuir*, vol. 27, no. 7, pp. 3451-3460, 2011/04/05 2011.
- [21] F. S. Taheri, A. Ghaemi, A. Maleki, and S. Shahhosseini, "High CO₂ Adsorption on Amine-Functionalized Improved Mesoporous Silica Nanotube as an Eco-Friendly Nanocomposite," *Energy & Fuels*, vol. 33, no. 6, pp. 5384-5397, 2019/06/20 2019.
- [22] S. Kazemi, A. Ghaemi, and K. Tahvildari, "Chemical absorption of carbon dioxide into aqueous piperazine solutions using a stirred reactor," (in en), *Iranian Journal of Chemistry and Chemical Engineering (IJCCE)*, 2019.
- [23] A. Ghaemi, Z. Jafari, and E. Etemad, "Prediction of CO₂ mass transfer flux in aqueous amine solutions using artificial neural networks," (in en), *Iranian Journal of Chemistry and Chemical Engineering (IJCCE)*, 2018.
- [24] R. Bera, M. Ansari, A. Alam, and N. Das, "Triptycene, Phenolic-OH, and Azo-Functionalized Porous Organic Polymers: Efficient and Selective CO₂ Capture," *ACS Applied Polymer Materials*, vol. 1, no. 5, pp. 959-968, 2019/05/10 2019.

- [25] B. Li, R. Gong, W. Wang, X. Huang, W. Zhang, H. Li, C. Hu, and B. Tan, "A New Strategy to Microporous Polymers: Knitting Rigid Aromatic Building Blocks by External Cross-Linker," *Macromolecules*, vol. 44, no. 8, pp. 2410-2414, 2011/04/26 2011.
- [26] B. Li, R. Gong, W. Wang, X. Huang, W. Zhang, H. Li, C. Hu, and B. J. M. Tan, "A new strategy to microporous polymers: knitting rigid aromatic building blocks by external cross-linker," vol. 44, no. 8, pp. 2410-2414, 2011.
- [27] G. Santori, M. Luberti, and H. Ahn, "Ideal adsorbed solution theory solved with direct search minimisation," *Computers & Chemical Engineering*, vol. 71, pp. 235-240, 2014/12/04/ 2014.



This article is an open-access article distributed under the terms and conditions of the Creative Commons Attribution (CC-BY) license.